HHS Public Access

Author manuscript

Obesity (Silver Spring). Author manuscript; available in PMC 2024 February 01.

Published in final edited form as:

Obesity (Silver Spring). 2023 February ; 31(2): 479–486. doi:10.1002/oby.23649.

Obesity and Metabolic Dysfunction Correlate with Background Parenchymal Enhancement in Premenopausal Women

Justin C. Brown[1,2,3], **Jennifer A. Ligibel**[4], **Tracy E. Crane**[5], **Despina Kontos**[6], **Shengping Yang**[1], **Emily F. Conant**[6], **Julie A. Mack**[7], **Rexford S. Ahima**[8], **Kathryn H. Schmitz**[7]

[1]Pennington Biomedical Research Center, 6400 Perkins Rd, Baton Rouge, LA 70808, USA

[2]LSU Health Sciences Center New Orleans School of Medicine, 1901 Perdido St, New Orleans, LA 70112, USA

[3]Stanley S. Scott Cancer Center, Louisiana State University Health Sciences Center, 533 Bolivar St, New Orleans, LA, 70112, USA

[4]Dana-Farber Cancer Institute, 450 Brookline Ave, Boston, MA 02215

[5]University of Miami, Miller School of Medicine, 1600 NW 10th Ave, Miami, FL 33136

[6]University of Pennsylvania, Perelman School of Medicine, 3400 Civic Center, Boulevard, Philadelphia, PA, 10104

[7]Penn State College of Medicine, 500 University Drive, Hershey, PA 17033

[8]Department of Medicine, Division of Endocrinology, Diabetes and Metabolism, Johns Hopkins University School of Medicine, 1830 E. Monument St., Baltimore, MD 21287

Abstract

Objective: This study tested the hypothesis that obesity and metabolic abnormalities correlate with background parenchymal enhancement (BPE)—the volume and intensity of enhancing fibroglandular breast tissue on dynamic contrast-enhanced magnetic resonance imaging (DCE-MRI).

Methods: Participants included 59 premenopausal women at high risk of breast cancer. Obesity was defined as a body mass index (BMI) ≥30 kg/m^2. Metabolic parameters included dual-energy x-ray absorptiometry-quantified body composition, plasma biomarkers of insulin resistance, adipokines, inflammation, and lipids, and urinary sex hormones. BPE was assessed using computerized algorithms on DCE-MRI.

Results: BMI was positively correlated with BPE (r=0.69; P<0.001); participants with obesity had higher BPE than those without obesity [404.9±189.6 *vs.* 261.8±143.8 cm^2; Δ: 143.1 cm^2 (95% CI: 49.5, 236.7); P=0.003]. Total body fat mass (r=0.68; P<0.001), body fat percentage (r=0.64; P<0.001), visceral adipose tissue area (r=0.65; P<0.001), subcutaneous adipose tissue area (r=0.60; P<0.001), insulin (r=0.59; P<0.001), glucose (r=0.35; P=0.011), the homeostatic model of insulin resistance (r=0.62; P<0.001); and leptin (r=0.60; P<0.001) were positively

Corresponding Author: Kathryn H. Schmitz, Ph.D., M.P.H., Penn State College of Medicine, 500 University Drive, Hershey, PA 17033, kzs95@psu.edu.

correlated with BPE. Adiponectin (r=−0.44; P<0.001) was negatively correlated with BPE. Plasma biomarkers of inflammation and lipids, and urinary sex hormones, were not correlated with BPE.

Conclusion: In premenopausal women at high risk of breast cancer, increased BPE is associated with obesity, insulin resistance, leptin, and adiponectin.

Keywords

adipokines; adipose tissue; breast cancer; inflammation; insulin resistance

INTRODUCTION

Background parenchymal enhancement (BPE) describes the volume and intensity of enhancing fibroglandular breast tissue on dynamic contrast-enhanced magnetic resonance imaging (DCE-MRI) (1, 2). BPE may be a radiomic biomarker of future breast cancer risk (3). Among 1,275 high-risk women undergoing DCE-MRI, BPE was associated with a 10-fold increase in breast cancer risk (4); this observation has been replicated with high BPE consistently predicting an increase in breast cancer risk (5, 6, 7). Established correlates of BPE are often not modifiable (e.g., age) or complex to modify (e.g., menopausal status) (8, 9, 10). The development of computerized methods to quantitatively measure BPE on DCE-MRI offers an opportunity to identify novel and modifiable correlates of BPE (11, 12, 13, 14, 15).

Obesity is a chronic, relapsing, progressive disease characterized by excess adiposity and metabolic dysfunction (16). The metabolic consequences of obesity include insulin resistance, alterations in the levels of adipokines, systemic inflammation, and abnormal lipid metabolism (17). High BPE reflects increased metabolic activity within the normal breast tissue, as evidenced by the correlation between higher standardized uptake value (SUV) on FDG-PET scan and higher BPE on MRI in women for whom both DCE-MRI and FDG-PET imaging is performed (18, 19). Therefore, it is possible that obesity and metabolic dysfunction may be related to BPE (8). These observations provided the scientific rationale for conducting an exploratory analysis to assess the associations of obesity and metabolic parameters with BPE in premenopausal women at high risk of breast cancer.

METHODS

Study Design

This cross-sectional analysis used the baseline data from the Women In Steady Exercise Research (WISER) Sister randomized clinical trial (20). The primary objective of the WISER Sister trial was to elucidate the hormonal mechanisms through which different doses of moderate-intensity aerobic exercise reduce breast cancer in high-risk premenopausal women. Detailed methods and the primary and secondary endpoints of the WISER Sister trial are published (20, 21, 22, 23, 24). The trial was conducted following Good Clinical Practice and the ethical principles originating in the Declaration of Helsinki. The Institutional Review Board approved the protocol and informed consent document at the University of Pennsylvania. All participants provided written informed consent. The study was registered on clinicaltrials.gov as NCT00892515. This report presents analyses not

prespecified in the statistical analysis plan of the study protocol; therefore, this *post hoc* analysis is hypothesis-generating.

Participants

Eligible participants were women with a predicted lifetime breast cancer risk ≥18%, defined as a previously-documented *BRCA* 1/2 mutation for the participant or their first-degree relative, or a Claus model predicted risk >18% (the Claus prediction was not calculated for women who lacked female first or second-degree relatives with breast cancer) (25), or a Gail model predicted risk >18% (the Gail prediction was not calculated for women age <35 y) (26). Additional eligibility criteria relevant to this analysis were a body mass index (BMI) of ≥21 to ≤50 kg/m^2; age 18–50 y; eumenorrheic (menstrual cycles 23–35 days in length); intact ovaries and uterus; self-reported consumption of ≤7 servings of alcoholic beverages weekly; self-reported participation of <75 minutes of aerobic exercise per week. Participants were excluded if they had evidence of an eating disorder assessed using the Eating Disorder Diagnostic Scale (27); had a personal history of cancer; were currently participating in a weight loss program; had current or recent prior use of hormonal contraceptives; or had any medical contraindication to exercise (28). Additional inclusion and exclusion details are published (20).

Obesity and Metabolic Parameters

Measures of obesity and metabolic parameters were obtained by trained staff who adhered to standardized procedures. Anthropometry included height (m) and body weight (kg), which were used to calculate BMI (kg/m^2). Obesity was defined as a BMI ≥30 kg/m^2. Body composition was measured using whole-body dual-energy x-ray absorptiometry (DXA; Hologic Inc). The densitometer was calibrated daily using whole-body tissue phantoms. All images were reviewed for quality assurance by a certified DXA technician. DXA was used to quantify total body fat mass (kg), body fat percentage (%), visceral adipose tissue area (cm^2), and subcutaneous adipose tissue area (cm^2) using APEX v.13.4 software. DXA is validated against body composition measures using computed tomography and magnetic resonance imaging (29, 30).

Blood was drawn between days six and ten of the menstrual cycle after overnight fasting, and serum and plasma samples were stored at −80°C. Fasting plasma glucose was measured using a spectrophotometric enzyme assay, and total cholesterol and triglycerides were measured using colorimetric assays on a COBAS C501 chemistry analyzer (Roche). Fasting insulin was quantified using a radioimmunoassay (EMD Millipore). Adiponectin and leptin were quantified using enzyme-linked immunosorbent assay (R&D Systems and Diagnostic System Labs, respectively). Chemokine ligand 2 (CCL2), interleukin 6 (IL-6), IL-10, IL-12, and tumor necrosis factor alpha (TNF-a) were quantified using a multiplex assay (MesoScale Discovery) (31). Blinded quality-control samples were interspersed among cases. The coefficients of variation for all samples were ≤10%. The homeostatic model assessment of insulin resistance (HOMA-IR) was calculated using fasting glucose and insulin (32).

All subjects provided first-morning urine samples daily for two menstrual cycles to quantify the urinary sex hormones. Microtiter plate competitive enzyme immunoassays were used to quantify the urinary metabolites of estrogen and progesterone [estrone-3-glucuronide (E1G) and pregnanediol-3-glucuronide (PdG)] (33). The secretion of these metabolites in the urine parallels serum concentrations of the parent hormones. All urine samples were corrected for specific gravity using a hand refractometer (NSG Precision Cells, Inc., Farmingdale, NY). The intra-assay coefficients of variation for E1G and PdG were ≤4.9% and ≤11.0%, respectively.

Background Parenchymal Enhancement

All participants completed DCE-MRI with dedicated surface breast coils between days six and ten of the menstrual cycle. Detailed methods to quantify BPE from DCE-MRI are published (34). Briefly, automated computational methods segmented the fibroglandular tissue (FGT) and the portion of the tissue enhancing (i.e., BPE) (11, 12, 13). Then, a clustering procedure formed voxel-wise FGT likelihood maps (12, 14). After FGT segmentation, voxel thresholding quantified BPE based on relative enhancement (13, 15).

Statistical Analysis

Descriptive characteristics in the overall study population are presented as means ± standard deviations for continuous variables and counts and proportions for categorical variables. The objective of this analysis was to use available data to examine our hypothesized conceptual model (Figure S1) by quantifying the strength of associations among obesity, metabolic dysregulation, and BPE. Measures of metabolic dysregulation were compared between participants with and without obesity using a *t*-test. The mean difference in BPE by obesity status is depicted graphically using a Gardner-Altman plot (35). The strength of the association between measures of metabolic dysregulation with BPE was quantified using the Pearson product-moment correlation coefficient (*r*) (36). We then calculated the correlation between measures of metabolic dysregulation and BPE adjusted for BMI (and vice versa), using the partial correlation coefficient from a multiple linear regression model (37). All statistical tests and *P* values are two-sided. Statistical analyses were conducted using Stata v.15.1 (StataCorp).

RESULTS

Baseline Characteristics

The average age of the 59 participants was 34.7±6.2 y (Table 1). All participants were at high risk of breast cancer; 18 had documented *BRCA* 1/2 mutations (30.5%), and the average Claus and Gail predicted breast cancer risks were 22.7±10.5% [range: 8.3–46.0%] and 22.7±8.4% [range: 11.6–49.7], respectively. The average BPE was 298.2±167.2 cm^2 [range: 17.5–774.8 cm^2].

Correlation of Obesity with Metabolic Dysregulation

The average BMI was 26.5±6.2 kg/m^2; 15 participants (25%) had obesity (e.g., BMI ≥30 kg/m^2). Participants with obesity had a profile of measures consistent with metabolic dysregulation (Table 2). Participants with obesity had excess total body fat mass [between

group difference (Δ): 22.0 kg (95% CI: 17.8, 26.2)], body fat percentage [Δ: 10.8% (95% CI: 7.9, 13.8)], visceral adipose tissue area [Δ: 102.8 cm^2 (95% CI: 80.7, 125.0)], and subcutaneous adipose tissue area [Δ: 285.2 cm^2 (95% CI: 226.1, 344.3)]. Participants with obesity had higher insulin [Δ: 4.1 uIU/mL (95% CI: 2.4, 5.8)], glucose [Δ: 19.8 mg/dL (95% CI: 7.0, 32.7)], and insulin resistance [Δ: 1.2 (95% CI: 0.8, 1.7)]. Participants with obesity had higher leptin [Δ: 20.1 ng/mL (95% CI: 14.1, 26.1)] and lower adiponectin [Δ: −6.2 mg/L (95% CI: −9.4, −2.9)]. Participants with obesity had higher CCL2 [Δ: 127.4 pg/mL (95% CI: 18.5, 236.2)], IL-6 [Δ: 3.4 (95% CI: 1.1, 5.6)], and TNF-a [Δ: 1.6 pg/mL (95% CI: 0.8, 2.4)] inflammatory biomarkers, but IL-10 and IL-12 were not statistically significantly different. Participants with obesity had higher triglycerides [Δ: 32.2 mg/dL (95% CI: 2.5, 61.9)] but cholesterol was not statistically significantly different. Participants with obesity had lower luteal phase progesterone [Δ: −40.1 ng/mL (95% CI: −65.4, −14.8)], but follicular phase progesterone and luteal and follicular phase estrogen were not statistically significantly different.

Correlation of Obesity and Metabolic Dysregulation with Background Parenchymal Enhancement

BMI was positively correlated with BPE (r=0.69; P<0.001); each 1 kg/m^2 increase in BMI was associated with an 18.4 cm^2 (95% CI: 13.1, 23.7) higher BPE (Figure S2). Participants with obesity had higher BPE than those without obesity [404.9±189.6 *vs.* 261.8±143.8; Δ: 143.1 cm^2 (95% CI: 49.5, 236.7); P=0.003; Figure 1]. Measures of adiposity and metabolic dysfunction were correlated with BPE (Table 3). Total body fat mass (r=0.68; P<0.001), body fat percentage (r=0.64; P<0.001), visceral adipose tissue area (r=0.65; P<0.001), and subcutaneous adipose tissue area (r=0.60; P<0.001) were positively correlated with BPE. Insulin (r=0.59; P<0.001), glucose (r=0.35; P=0.011), and insulin resistance (r=0.62; P<0.001) were all positively correlated with BPE. Leptin, a measure of adiposity, was also positively correlated with BPE (r=0.60; P<0.001). Adiponectin was negatively correlated with BPE (r= −0.44; P<0.001). Plasma inflammatory biomarkers, e.g., CCL2, IL-6, IL-10, IL-12, and TNF-a, and lipids were not associated with BPE. Urinary sex hormones, e.g., E1G and PdG, were not associated with BPE.

The correlations between BPE and measures of adiposity and metabolic dysfunction were attenuated after adjusting for the BMI (the hypothesized cause of metabolic dysfunction) and were no longer statistically significantly associated with BPE. A similar analysis that adjusted the association between the BMI and BPE for measures of metabolic dysregulation (the hypothesized mediator) demonstrated that the BMI remained a statistically significant correlate of BPE, except when adjusted for the total fat mass [(r=0.17; P=0.20); Table S1].

DISCUSSION

The major finding of this exploratory cross-sectional analysis is that obesity and metabolic dysfunction correlate with BPE in premenopausal women at high risk of breast cancer. BMI was positively correlated with BPE, and women with obesity had significantly higher BPE than those without obesity. The amount and location of adiposity and biomarkers of metabolic dysregulation, including insulin resistance and adipokine imbalance, correlated

with BPE. Obesity and associated insulin resistance and changes in adipokines can be modified by lifestyle, medical, or surgical treatments; thus, it is plausible that treating obesity and correcting metabolic dysfunction may reduce BPE in women at high risk of breast cancer.

Our findings are consistent with prior studies that report BMI was associated with qualitative BPE (e.g., visual assessment categories for BPE: minimal, mild, moderate, or marked) (8, 9, 10). In a meta-analysis of 18 studies, women with at least moderate BPE enhancement had a 1.6 higher odds of breast cancer, and women with at least mild BPE enhancement had a 2.1 higher odds of breast cancer (38). These observations indicate that modest differences in BMI—the equivalent of ~5–8 kg of body weight for the average U.S. woman—may have a potentially clinically meaningful impact on BPE and subsequent breast cancer risk.

Obesity is well known to be positively associated with insulin resistance and leptin, and inversely correlated with adiponectin (39). We propose that these metabolic changes may be key determinants of the link between obesity and BPE. In our statistical models that adjusted for BMI, no measures of metabolic dysregulation remained correlated with BPE. Although these data are cross-sectional, this observation is consistent with our hypothesized conceptual model that obesity is a common cause of metabolic dysregulation.

The novel finding that obesity and abnormal metabolic parameters are correlated with BPE provides potential support to observational studies that link obesity and metabolic dysregulation to breast cancer risk in premenopausal women. These findings are consistent with reports that demonstrate abdominal adiposity may be associated with a higher risk of breast cancer in *BRCA* 1/2 carriers and premenopausal women (40). Obesity-related metabolic dysfunction, such as hyperinsulinemia, is also associated with an increased risk of premenopausal breast cancer (41). Conversely, weight loss in early adulthood is associated with a reduced risk of breast cancer in *BRCA* 1/2 carriers (42). These data extend our knowledge by linking obesity and metabolic dysregulation to an objective radiologic measure of breast physiology that is strongly predictive of breast cancer in high-risk women.

Inflammatory biomarkers, lipids, and urinary sex hormones were not correlated with BPE. A prior report in postmenopausal women identified a correlation between serum estrogen and estradiol (43). It is plausible that we did not detect this association because we measured sex hormone concentrations in the urine and our participants were premenopausal women. Among *BRCA* 1/2 mutation carriers, breast tissues express dysregulated lipid metabolism (44). This area warrants future investigation as dysregulated lipid metabolism may have important therapeutic implications for cancer prevention (45). Contrary to our hypothesis, inflammation was not correlated with BPE. The reasons for this lack of correlation are unclear; additional research is needed to replicate our findings and interrogate this hypothesis.

Multimodal lifestyle interventions that integrate dietary modification and increased physical activity are the foundation of obesity care (46). Multimodal lifestyle interventions achieve 3–5% weight loss and correct many metabolic consequences of ectopic adiposity, including insulin resistance, adipokine dysfunction, systemic inflammation, and lipid metabolism

(17). We have previously reported that moderate-intensity aerobic exercise reduces BPE in high-risk premenopausal women (21), with effects potentially mediated by reductions in visceral adipose tissue (22). Emerging data indicate that novel dietary approaches, such as time-restricted eating, confer unique metabolic benefits, such as improved insulin sensitivity, without substantively reducing body weight (47). Time-restricted eating in preclinical models reduces mammary tumor growth, and this effect is mediated by the normalization of hyperinsulinemia (48). However, it is unknown if novel dietary strategies, such as time-restricted eating, reduce BPE in women at high risk of breast cancer.

There are several limitations to our study. The statistical analyses reported here were not prespecified in the statistical analysis plan. Readers should therefore interpret these data as hypothesis-generating. This study used a cross-sectional design, and thus we cannot comment on the temporal sequences. The observational design precludes our ability to identify causal relationships, and the reported associations may result from unmeasured confounding. We utilized all available data to support our conceptual model; however additional longitudinal data are needed to substantiate the causality and reversibility of these hypothesized relationships. The participants included in our analysis were premenopausal women who were at high risk of breast cancer. It is unknown if our findings can be generalized to postmenopausal women or premenopausal women at average risk of breast cancer.

Nonetheless, there are several strengths to our study. The study participants included premenopausal women at high risk of breast cancer. This group is a small yet highly vulnerable subgroup of the population. Participants in this study were recruited from throughout the United States, which may improve the generalizability of our findings. The methods for assessing obesity and metabolic dysfunction data included measurement of body composition using DXA and plasma biomarkers. Our outcome data for BPE was obtained using rigorous DCE-MRI methods and quantified using objective computerized algorithms that have been validated and are reproducible.

CONCLUSION

In premenopausal women at high risk of breast cancer, obesity and metabolic dysfunction were correlated with higher levels of quantitatively measured BPE. Our results provide foundational data for the hypothesis that treating obesity and related insulin resistance and adipokine abnormalities may reduce BPE and breast cancer risk. Randomized controlled trials are necessary to test this hypothesis.

Supplementary Material

Refer to Web version on PubMed Central for supplementary material.

Funding

JCB is supported by grants from the National Institutes of Health and the American Institute for Cancer Research. JAL is supported by grants from the National Institutes of Health and the Susan G. Komen Foundation. TEC is supported by grants from the National Institutes of Health and the Patient-Centered Outcomes Research Institute.

RSA is supported by Bloomberg Distinguished Professorship. KHS is supported by grants from the National Institutes of Health. No other authors acknowledge relevant financial support.

Disclosure

EFC is on the advisory panels and receives funding from Hologic, Inc. and iCAD, Inc. No other authors disclose any relevant conflicts of interest.

REFERENCES

1. Arasu VA, Miglioretti DL, Sprague BL, Alsheik NH, Buist DSM, Henderson LM, et al. Population-Based Assessment of the Association Between Magnetic Resonance Imaging Background Parenchymal Enhancement and Future Primary Breast Cancer Risk. J Clin Oncol 2019;37: 954–963. [PubMed: 30625040]
2. King V, Gu Y, Kaplan JB, Brooks JD, Pike MC, Morris EA. Impact of menopausal status on background parenchymal enhancement and fibroglandular tissue on breast MRI. Eur Radiol 2012;22: 2641–2647. [PubMed: 22752463]
3. Liao GJ, Henze Bancroft LC, Strigel RM, Chitalia RD, Kontos D, Moy L, et al. Background parenchymal enhancement on breast MRI: A comprehensive review. Journal of Magnetic Resonance Imaging 2020;51: 43–61. [PubMed: 31004391]
4. King V, Brooks JD, Bernstein JL, Reiner AS, Pike MC, Morris EA. Background parenchymal enhancement at breast MR imaging and breast cancer risk. Radiology 2011;260: 50–60. [PubMed: 21493794]
5. Grimm LJ, Saha A, Ghate SV, Kim C, Soo MS, Yoon SC, et al. Relationship between Background Parenchymal Enhancement on High-risk Screening MRI and Future Breast Cancer Risk. Acad Radiol 2019;26: 69–75. [PubMed: 29602724]
6. Dontchos BN, Rahbar H, Partridge SC, Korde LA, Lam DL, Scheel JR, et al. Are Qualitative Assessments of Background Parenchymal Enhancement, Amount of Fibroglandular Tissue on MR Images, and Mammographic Density Associated with Breast Cancer Risk? Radiology 2015;276: 371–380. [PubMed: 25965809]
7. Pike MC, Pearce CL. Mammographic density, MRI background parenchymal enhancement and breast cancer risk. Ann Oncol 2013;24 Suppl 8: viii37–viii41. [PubMed: 24131968]
8. Hruska CB, Rhodes DJ, Conners AL, Jones KN, Carter RE, Lingineni RK, et al. Background parenchymal uptake during molecular breast imaging and associated clinical factors. AJR Am J Roentgenol 2015;204: W363–370. [PubMed: 25714323]
9. Hellgren R, Saracco A, Strand F, Eriksson M, Sundbom A, Hall P, et al. The association between breast cancer risk factors and background parenchymal enhancement at dynamic contrast-enhanced breast MRI. Acta Radiol 2020;61: 1600–1607. [PubMed: 32216451]
10. Brooks JD, Christensen RAG, Sung JS, Pike MC, Orlow I, Bernstein JL, et al. MRI background parenchymal enhancement, breast density and breast cancer risk factors: A cross-sectional study in pre- and post-menopausal women. NPJ Breast Cancer 2022;8: 97. [PubMed: 36008488]
11. Wu S, Weinstein SP, Conant EF, Schnall MD, Kontos D. Automated chest wall line detection for whole-breast segmentation in sagittal breast MR images. Medical physics 2013;40: 042301. [PubMed: 23556914]
12. Wu S, Weinstein SP, Conant EF, Kontos D. Automated fibroglandular tissue segmentation and volumetric density estimation in breast MRI using an atlas-aided fuzzy C-means method. Medical physics 2013;40: 122302. [PubMed: 24320533]
13. Wei D, Jahani N, Cohen E, Weinstein S, Hsieh MK, Pantalone L, et al. Fully automatic quantification of fibroglandular tissue and background parenchymal enhancement with accurate implementation for axial and sagittal breast MRI protocols. Medical physics 2021;48: 238–252. [PubMed: 33150617]
14. Wu S, Weinstein S, Kontos D. Atlas-based probabilistic fibroglandular tissue segmentation in breast MRI. Medical image computing and computer-assisted intervention : MICCAI International Conference on Medical Image Computing and Computer-Assisted Intervention 2012;15: 437–445. [PubMed: 23286078]

15. Wu S, Weinstein SP, DeLeo MJ 3rd, Conant EF, Chen J, Domchek SM, et al. Quantitative assessment of background parenchymal enhancement in breast MRI predicts response to risk-reducing salpingo-oophorectomy: preliminary evaluation in a cohort of BRCA1/2 mutation carriers. Breast cancer research : BCR 2015;17: 67. [PubMed: 25986460]
16. Bray GA, Kim KK, Wilding JPH, World Obesity F. Obesity: a chronic relapsing progressive disease process. A position statement of the World Obesity Federation. Obes Rev 2017;18: 715–723. [PubMed: 28489290]
17. Heymsfield SB, Wadden TA. Mechanisms, Pathophysiology, and Management of Obesity. N Engl J Med 2017;376: 254–266. [PubMed: 28099824]
18. An YS, Jung Y, Kim JY, Han S, Kang DK, Park SY, et al. Metabolic Activity of Normal Glandular Tissue on (18)F-Fluorodeoxyglucose Positron Emission Tomography/Computed Tomography: Correlation with Menstrual Cycles and Parenchymal Enhancements. J Breast Cancer 2017;20: 386–392. [PubMed: 29285044]
19. Leithner D, Baltzer PA, Magometschnigg HF, Wengert GJ, Karanikas G, Helbich TH, et al. Quantitative Assessment of Breast Parenchymal Uptake on 18F-FDG PET/CT: Correlation with Age, Background Parenchymal Enhancement, and Amount of Fibroglandular Tissue on MRI. J Nucl Med 2016;57: 1518–1522. [PubMed: 27230924]
20. Schmitz KH, Williams NI, Kontos D, Kurzer MS, Schnall M, Domchek S, et al. Women In Steady Exercise Research (WISER) Sister: study design and methods. Contemp Clin Trials 2015;41: 17–30. [PubMed: 25559914]
21. Schmitz KH, Williams NI, Kontos D, Domchek S, Morales KH, Hwang WT, et al. Dose-response effects of aerobic exercise on estrogen among women at high risk for breast cancer: a randomized controlled trial. Breast Cancer Res Treat 2015;154: 309–318. [PubMed: 26510851]
22. Brown JC, Kontos D, Schnall MD, Wu S, Schmitz KH. The Dose-Response Effects of Aerobic Exercise on Body Composition and Breast Tissue among Women at High Risk for Breast Cancer: A Randomized Trial. Cancer Prev Res (Phila) 2016;9: 581–588. [PubMed: 27099272]
23. Sturgeon K, Digiovanni L, Good J, Salvatore D, Fenderson D, Domchek S, et al. Exercise-Induced Dose-Response Alterations in Adiponectin and Leptin Levels Are Dependent on Body Fat Changes in Women at Risk for Breast Cancer. Cancer Epidem Biomar 2016;25: 1195–1200.
24. Ehret CJ, Zhou S, Tchou JC, Schmitz KH, Sturgeon KM. Dose-dependent effects of aerobic exercise on clinically relevant biomarkers among healthy women at high genetic risk for breast cancer: A secondary analysis of a randomized controlled study. Cancer Rep (Hoboken) 2022;5: e1497. [PubMed: 34240819]
25. Claus EB, Risch N, Thompson WD. Autosomal dominant inheritance of early-onset breast cancer. Implications for risk prediction. Cancer 1994;73: 643–651. [PubMed: 8299086]
26. Gail MH, Brinton LA, Byar DP, Corle DK, Green SB, Schairer C, et al. Projecting individualized probabilities of developing breast cancer for white females who are being examined annually. J Natl Cancer Inst 1989;81: 1879–1886. [PubMed: 2593165]
27. Stice E, Telch CF, Rizvi SL. Development and validation of the Eating Disorder Diagnostic Scale: a brief self-report measure of anorexia, bulimia, and binge-eating disorder. Psychol Assess 2000;12: 123–131. [PubMed: 10887758]
28. Medicine ACoS. ACSM's Guidelines for Exercise Testing and Prescription. Lippincott Williams & Wilkins: Philadelphia, PA, 2013.
29. Shepherd JA, Ng BK, Sommer MJ, Heymsfield SB. Body composition by DXA. Bone 2017;104: 101–105. [PubMed: 28625918]
30. Toombs RJ, Ducher G, Shepherd JA, De Souza MJ. The impact of recent technological advances on the trueness and precision of DXA to assess body composition. Obesity (Silver Spring) 2012;20: 30–39. [PubMed: 21760631]
31. Chowdhury F, Williams A, Johnson P. Validation and comparison of two multiplex technologies, Luminex and Mesoscale Discovery, for human cytokine profiling. J Immunol Methods 2009;340: 55–64. [PubMed: 18983846]
32. Levy JC, Matthews DR, Hermans MP. Correct homeostasis model assessment (HOMA) evaluation uses the computer program. Diabetes Care 1998;21: 2191–2192. [PubMed: 9839117]

33. Munro CJ, Stabenfeldt G, Cragun J, Addiego L, Overstreet J, Lasley B. Relationship of serum estradiol and progesterone concentrations to the excretion profiles of their major urinary metabolites as measured by enzyme immunoassay and radioimmunoassay. Clinical chemistry 1991;37: 838–844. [PubMed: 2049848]
34. Boston RC, Schnall MD, Englander SA, Landis JR, Moate PJ. Estimation of the content of fat and parenchyma in breast tissue using MRI T1 histograms and phantoms. Magn Reson Imaging 2005;23: 591–599. [PubMed: 15919606]
35. Ho J, Tumkaya T, Aryal S, Choi H, Claridge-Chang A. Moving beyond P values: data analysis with estimation graphics. Nat Methods 2019;16: 565–566. [PubMed: 31217592]
36. Pearson K VII. Mathematical contributions to the theory of evolution.—III. Regression, heredity, and panmixia. Philosophical Transactions of the Royal Society of London Series A, containing papers of a mathematical or physical character 1896: 253–318.
37. Greene WH. Econometric analysis. Pearson Education India, 2003.
38. Thompson CM, Mallawaarachchi I, Dwivedi DK, Ayyappan AP, Shokar NK, Lakshmanaswamy R, et al. The Association of Background Parenchymal Enhancement at Breast MRI with Breast Cancer: A Systematic Review and Meta-Analysis. Radiology 2019;292: 552–561. [PubMed: 31237494]
39. Ahima RS, Flier JS. Adipose tissue as an endocrine organ. Trends Endocrinol Metab 2000;11: 327–332. [PubMed: 10996528]
40. Harvie M, Hooper L, Howell AH. Central obesity and breast cancer risk: a systematic review. Obes Rev 2003;4: 157–173. [PubMed: 12916817]
41. Del Giudice ME, Fantus IG, Ezzat S, McKeown-Eyssen G, Page D, Goodwin PJ. Insulin and related factors in premenopausal breast cancer risk. Breast Cancer Res Treat 1998;47: 111–120. [PubMed: 9497099]
42. Kotsopoulos J, Olopado OI, Ghadirian P, Lubinski J, Lynch HT, Isaacs C, et al. Changes in body weight and the risk of breast cancer in BRCA1 and BRCA2 mutation carriers. Breast Cancer Res 2005;7: R833–843. [PubMed: 16168130]
43. Brooks JD, Sung JS, Pike MC, Orlow I, Stanczyk FZ, Bernstein JL, et al. MRI background parenchymal enhancement, breast density and serum hormones in postmenopausal women. Int J Cancer 2018;143: 823–830. [PubMed: 29524207]
44. Ramadan S, Arm J, Silcock J, Santamaria G, Buck J, Roy M, et al. Lipid and Metabolite Deregulation in the Breast Tissue of Women Carrying BRCA1 and BRCA2 Genetic Mutations. Radiology 2015;275: 675–682. [PubMed: 25734415]
45. Bian X, Liu R, Meng Y, Xing D, Xu D, Lu Z. Lipid metabolism and cancer. J Exp Med 2021;218.
46. Jensen MD, Ryan DH, Apovian CM, Ard JD, Comuzzie AG, Donato KA, et al. 2013 AHA/ACC/TOS Guideline for the Management of Overweight and Obesity in Adults. Circulation 2014;129: S102–S138. [PubMed: 24222017]
47. Gabel K, Varady KA. Current research: effect of time restricted eating on weight and cardiometabolic health. J Physiol 2020.
48. Das M, Ellies LG, Kumar D, Sauceda C, Oberg A, Gross E, et al. Time-restricted feeding normalizes hyperinsulinemia to inhibit breast cancer in obese postmenopausal mouse models. Nat Commun 2021;12: 565. [PubMed: 33495474]

STUDY IMPORTANCE

What is already known?

- Background parenchymal enhancement (BPE)—the volume and intensity of enhancing fibroglandular breast tissue on dynamic contrast-enhanced magnetic resonance imaging (DCE-MRI)—predicts up to a 10-fold increase in breast cancer risk.
- Higher levels of BPE reflect increased metabolic activity within the breast tissue.

What does this study add?

- Body mass index was positively correlated with BPE; participants with obesity had higher BPE than those without obesity.
- Body composition and biomarkers of insulin resistance and adipokines were correlated with BPE.
- Plasma biomarkers of inflammation and lipids, and urinary sex hormones, were not correlated with BPE.

How might these results change the direction of research or the focus of clinical practice?

- These data support the hypothesis that treating obesity and related insulin resistance and adipokine abnormalities may reduce BPE.

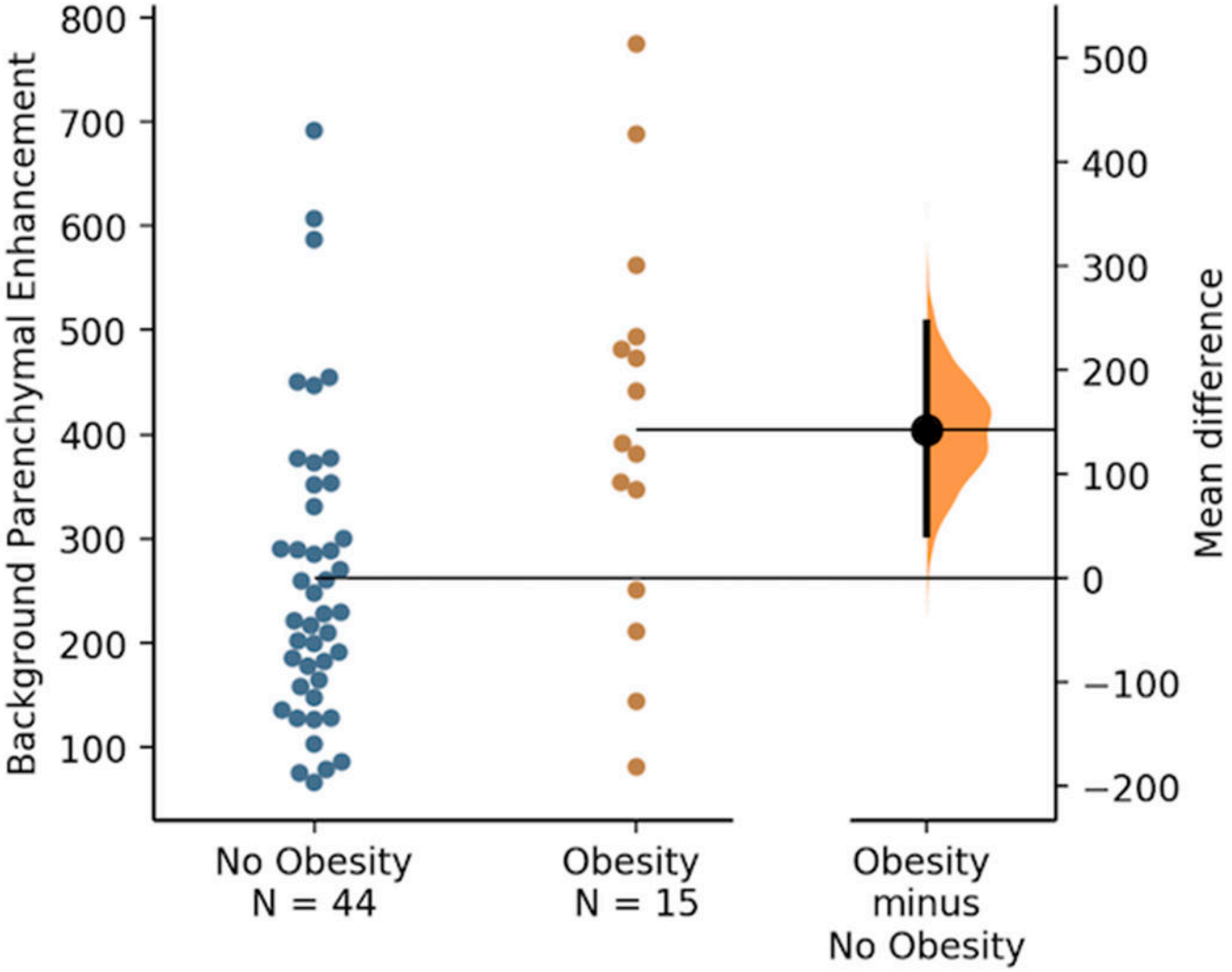

Figure 1.
Background parenchymal enhancement (cm^2) by obesity status

Table 1.

Baseline characteristics of the study population

Characteristic	(*N* = 59)
Age, y	34.7±6.2
BRCA gene mutation status, *n* (%)	
Positive	18 (30.5%)
Negative	7 (11.9%)
Not tested	34 (57.6%)
Predicted breast cancer risk, %	
Gail model[a] (*n* = 28)	22.7±8.4
Claus model[b] (*n* = 53)	22.7±10.5
Age at menarche, y	12.6±1.2
Children, n (%)	
Yes	32 (54.2%)
No	24 (40.7%)
Missing	3 (5.1%)
Background parenchymal enhancement, cm^2	298.2±167.2

[a]Gail prediction is not calculated for women below the age of 35.

[b]Claus prediction is not calculated for women who lack female first or second-degree relatives with breast cancer.

Values are mean ± standard deviation or *n* (%).

Table 2.

Measures of metabolic dysregulation in the overall study population and stratified by obesity status

Metabolic dysregulation	Overall (*N* = 59)	Obesity (*n* = 15; 25%)	No Obesity (*n* = 44; 75%)	*P*
Body mass index, kg/m^2	26.5±6.2	36.6±3.6	23.7±3.3	<0.001
Fat mass, kg	28.1±11.1	45.4±7.8	23.4±6.0	<0.001
Body fat, %	37.4±6.3	45.9±3.2	35.1±4.7	<0.001
Visceral adipose tissue, cm^2	81.6±54.2	162.4±37.7	59.6±32.8	<0.001
Subcutaneous adipose tissue, cm^2	341.6±148.3	565.7±92.7	280.5±90.0	<0.001
Insulin, uIU/mL	4.8±3.0	8.0±3.2	3.9±2.3	<0.001
Glucose, mg/dL	84.2±20.4	99.9±31.5	80.1±14.2	0.003
HOMA-IR	1.0±0.8	2.0±1.1	0.8±0.5	<0.001
Leptin, ng/mL	18.7±12.4	34.5±8.7	14.4±9.4	<0.001
Adiponectin, mg/L	12.1±5.6	7.3±2.2	13.5±5.5	<0.001
CCL2, pg/mL	181.8±178.0	279.1±353.7	151.7±34.4	0.023
IL-6, pg/mL	4.5±3.6	7.1±4.2	3.8±3.1	0.005
IL-10, pg/mL	3.2±1.2	3.4±0.8	3.1±1.3	0.52
IL-12, pg/mL	1.9±1.1	2.1±0.8	1.9±1.1	0.48
TNF-a, pg/mL	4.9±1.4	6.2±1.5	4.6±1.2	<0.001
Total cholesterol, mg/dL	192.0±36.6	196.4±35.9	190.8±37.1	0.66
Triglycerides, mg/dL	88.9±45.2	114.4±31.6	82.2±46.1	0.034
Estrogen, ng/mL				
Follicular	790.0±401.9	725.0±394.3	806.3±406.7	0.55
Luteal	480.3±259.9	327.5±121.4	518.5±271.9	0.28
Progesterone, ng/mL				
Follicular	26.5±14.9	20.7±19.1	27.9±13.5	0.15
Luteal	71.0±40.5	38.9±21.9	79.0±40.2	0.003

Values are mean ± standard deviation.

HOMA-IR, homeostatic model of insulin resistance; CCL2, chemokine ligand 2; IL-6, interleukin-6; IL-10, interluekin-10; IL-12, interleukin-12; TNF-a, tumor necrosis factor-alpha.

Table 3.

Correlation between measures of metabolic dysregulation and background parenchymal enhancement, with and without adjustment for body mass index

	Without Adjustment for Body Mass Index		With Adjustment for Body Mass Index	
Metabolic dysregulation	***r***	***P***	***r***	***P***
Fat mass	0.68	<0.001	0.05	0.69
Body fat	0.64	<0.001	0.08	0.56
Visceral adipose tissue	0.65	<0.001	0.12	0.38
Subcutaneous adipose tissue	0.60	<0.001	−0.21	0.12
Insulin	0.59	<0.001	0.23	0.097
Glucose	0.35	0.011	0.08	0.59
HOMA-IR	0.62	<0.001	0.26	0.062
Leptin	0.60	<0.001	0.08	0.58
Adiponectin	−0.44	<0.001	−0.12	0.37
CCL2	0.07	0.61	−0.08	0.58
IL-6	0.17	0.21	−0.15	0.30
IL-10	−0.01	0.96	−0.07	0.61
IL-12	−0.16	0.25	−0.21	0.13
TNF-a	0.10	0.46	−0.11	0.41
Total cholesterol	0.05	0.71	−0.01	0.96
Triglycerides	0.20	0.16	−0.13	0.36
Estrogen				
Follicular	−0.05	0.69	−0.11	0.44
Luteal	−0.13	0.33	0.07	0.64
Progesterone				
Follicular	−0.08	0.56	−0.01	0.99
Luteal	−0.17	0.22	0.17	0.22

HOMA-IR, homeostatic model of insulin resistance; CCL2, chemokine ligand 2; IL-6, interleukin-6; IL-10, interleukin-10; IL-12, interleukin-12; TNF-a, tumor necrosis factor-alpha.